Microwave Nondestructive Testing Using Multi-Frequency Near-Field Sensors

Yuki Gao, *Member, IEEE*, and Reza K. Amineh, *Senior Member, IEEE*

***Abstract*—This project is focused on microwave imaging and sensing of dielectric materials. An array of microwave sensors with each element of the array resonating at different frequency is utilized. The array of microwave sensors operates within the range of 1 GHz to 10 GHz. This frequency band allows for data acquisition with cost-effect microwave circuitry that can replace costly vector network analyzers (VNA) for measurements. Although the frequency is relatively low for high resolution imaging, the acquisition of the evanescent waves in extreme proximity to the imaged object and processing of these waves using near-field holographic imaging allows for obtaining high resolution in cross-range direction. This new imaging and scanning system can be utilized for nondestructive testing (NDT) of multilayer composite materials, PCB testing, and even skin cancer diagnosis.**

***Index Terms*—Microwave imaging, nondestructive testing (NDT), nonmetallic materials, PCB testing.**

I. Introduction

NONMETALLIC materials such as flat substrates are employed in various industrial sectors due to advantages such as low cost, lightweight, and resistance to corrosion. However, there may be defects and delaminations that are undesirable. Therefore, it is critical to detect the unwanted factors via nondestructive testing (NDT) techniques.

For instance, the electronic industry is concerned about delamination in composite materials that are used for PCB substrates because the formation of defects may lead to the deterioration of the material strength [1]. In addition, NDT inspections of critical aircraft components with corrosions that are hidden under the paint cannot be detected visually [2].

Therefore, detecting and acquiring defects and their thickness is extremely important. However, traditional NDT techniques may not be able to assess composites. Thus, an array of sensors resonating at multiple frequencies will be utilized for assessing the size of defects. The responses obtained from the sensor are later processed through a robust method. Noted, the sensor used for this proposed method is adapted from [3]. Simulation and experimental results are shown to demonstrate the performance of the proposed method.

II. Theory

Here, we briefly review the theory of near-field holographic imaging with multi-frequency near-field sensor where multiple frequency data are used for imaging the defects in nonmetallic media.

Fig. 1 illustrates the proposed microwave holographic imaging setup that consists of a multi-frequency near-field sensor and collects backscattered data over a rectangular aperture. The data acquisition and image reconstruction are performed over flat surfaces (along x and y axes) at various z-planes. Also, the scattered field is recorded by the sensor at each position (x, y). Such scattered response is acquired from subtracting the responses without defects from the responses with defects. The image reconstruction process is aimed at providing images at $z = z_i$ planes, where $i = 1, \dots, N_z$. The complex-valued scattered field $E^{SC}(x, y)$, is measured at each sampling position, at N_ω frequencies within the band of ω_1 to ω_{N_ω}, by the sensor. Also, it is worth noting that the imaging system is assumed to be linear and space-invariant (LSI).

First, the point-spread functions (PSFs) of the LSI imaging system are obtained *a priori*. These PSFs are denoted by $E^{SC,PD}$ and are approximated by measuring small defects called point-wise defects (PDs) placed on each imaged plane one at a time. The scattered response recorded for the PD placed on the i-th layer is denoted by $E_i^{SC,PD}(x, y)$. Then, according to the convolution theory, the defects' response for each imaged plane, $E_i^{SC}(x, y)$, can be written as the convolution of the collected PSF for that plane, $E_i^{SC,PD}(x, y)$, with the contrast function of the defect on the corresponding plane $f_i(x, y)$. Next, the response due to the defects on material under test (MUT), $E^{SC}(x, y)$, can be obtained from the superposition of the responses of all the imaged planes, $E_i^{SC}(x, y)$, where $i = 1, \dots, N_z$, as:

$$E^{SC}(x, y) = \sum_{i=1}^{N_z} E_i^{SC}(x, y) = \sum_{i=1}^{N_z} E_i^{SC,PD}(x, y) *_x *_y f_i(x, y) \tag{1}$$

Here, $*_x$ and $*_y$ denote convolution along x and y, respectively. By having (1) at multiple frequencies, and applying discrete time Fourier transform (DTFT) along the x and y directions we obtain the following system of equations at each $\boldsymbol{\kappa} = (k_x, k_y)$:

$$\underline{\tilde{\tilde{\mathbf{E}}}}^{SC} = \underline{\underline{\tilde{\tilde{\mathbf{D}}}}}\,\underline{\tilde{\tilde{\mathbf{F}}}} \tag{2}$$

where

$$\underline{\tilde{\tilde{\mathbf{E}}}}^{SC} = \begin{bmatrix} \tilde{\tilde{E}}^{SC}(\boldsymbol{\kappa}, \omega_1) \\ \vdots \\ \tilde{\tilde{E}}^{SC}(\boldsymbol{\kappa}, \omega_{N_\omega}) \end{bmatrix},$$

The authors are with the Department of Electrical and Computer Engineering, New York Institute of Technology, New York, NY 10023 USA.

$$\tilde{\tilde{\underline{\mathbf{D}}}} = \begin{bmatrix} \tilde{\tilde{E}}_1^{SC,PD}(\boldsymbol{\kappa},\omega_1) & \cdots & \tilde{\tilde{E}}_{N_z}^{SC,PD}(\boldsymbol{\kappa},\omega_1) \\ \vdots & \ddots & \vdots \\ \tilde{\tilde{E}}_1^{SC,PD}(\boldsymbol{\kappa},\omega_{N_\omega}) & \cdots & \tilde{\tilde{E}}_{N_z}^{SC,PD}(\boldsymbol{\kappa},\omega_{N_\omega}) \end{bmatrix}, \; \tilde{\tilde{\underline{\mathbf{F}}}} = \begin{bmatrix} \tilde{\tilde{f}}_1(\boldsymbol{\kappa}) \\ \vdots \\ \tilde{\tilde{f}}_{N_z}(\boldsymbol{\kappa}) \end{bmatrix} \quad (3)$$

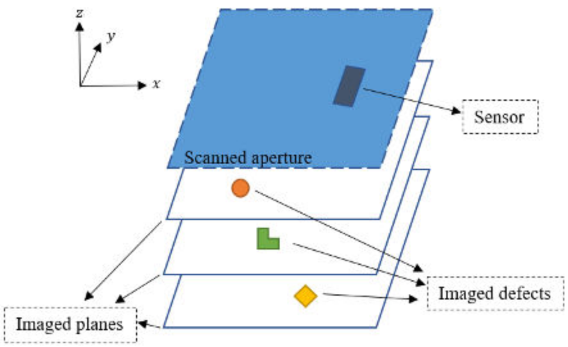

Fig. 1. Illustration of microwave holographic imaging setup.

Fig. 2. Multi-frequency near-field sensor.

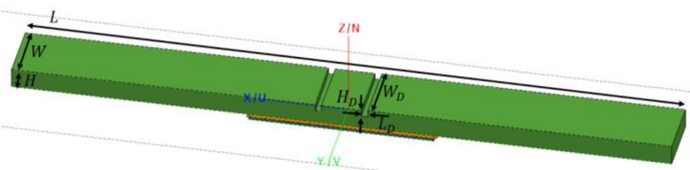

Fig. 3. Illustration of the simulation setup in FEKO software.

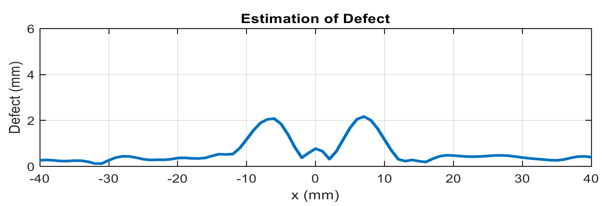

Fig. 4. Depth estimation of defects with size of 2 mm.

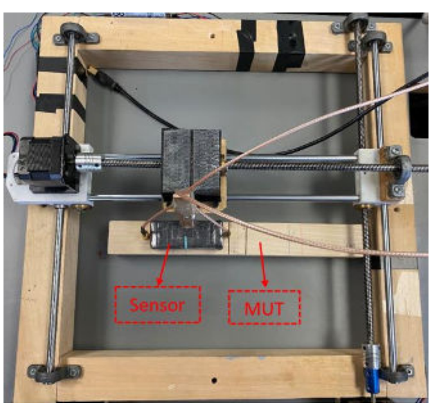

Fig. 5. Main components of the microwave imaging system.

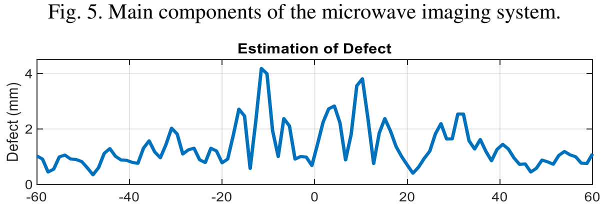

Fig. 6. Depth estimation of defects with size of 4 mm.

and $\tilde{\tilde{E}}^{SC}(\boldsymbol{\kappa},\omega_n)$, $\tilde{\tilde{E}}_i^{SC,PD}(\boldsymbol{\kappa},\omega_n)$, and $\tilde{\tilde{f}}_i(\boldsymbol{\kappa})$ are DTFT of $E^{SC}(x,y,\omega_n)$, $E_i^{SC,PD}(x,y,\omega_n)$, and $f_i(x,y)$. After solving all the systems of equations, to obtain $\tilde{\tilde{f}}_i(\boldsymbol{\kappa})$, we apply inverse DTFT to reconstruct images $f_i(x,y)$. For a more detailed explanation of the theory, please refer to [4].

III. Simulation and Experimental Results

In this section, simulation and experimental results are presented. A sensor array with five elements of the array resonating within the frequency range of 1 to 10 GHz [3] shown in Fig. 2 is employed for both studies. For faster data acquisition, one dimensional (1D) scanning of the array was performed.

Fig. 3 illustrates the setup where the composite substrate is 1 mm above the sensor and the defects are at positions of $(\pm 7\text{ mm}, 0)$, with length of L_D= 2 mm, width of W_D= 20 mm, and depth of H_D= 2 mm. The composite is assumed to have a relative permittivity of $\varepsilon_r = 4$ and a loss tangent of 0.0001. After applying the holographic imaging process, the total depths of the defects are obtained by summing the normalized reconstructed images. Fig. 4 illustrates the estimation of defects with actual depths of 2 mm where the estimation is close to 2 mm.

Next, Fig. 5 shows the microwave imaging system that consists of a rectangular scanning system, MUT (wood), and a sensor. Fig. 6 illustrates the estimation of the defects with actual depth of 4 mm and positions of $(\pm 10\text{ mm}, 0)$. The true dimensions of the defects are length of 1 mm, width of 5 mm, and depth of 4 mm. It is observed that the estimated values are close to the actual depths.

IV. Conclusion and Future Career Plans

For the first time, the use of multi-frequency near-field sensor is extended for microwave imaging of nonmetallic substrates. In general, defects can be detected and estimated in simulation and experimental studies. Furthermore, we conducted simulation studies with skin tissues and verified that the proposed methodology can be employed for skin tumor imaging.

Moving forward, I would like to explore the career opportunities in the fields of microwave and RF and pursue a PhD degree in this area. Lastly, I am excited to attend IMS 2022 at Denver, Colorado.

Acknowledgment

I would like to thank IEEE MTT-S Undergraduate/Pre-Graduate Scholarship and Dr. Amineh for supporting and motivating me to continue my research in this field.

References

[1] V. R. Samsingh, S. Subbaraj, K. Malathi, E. F. Sundarsingh, P. Yogeshwari, K. Saffrine, and Y. V. R. Rao, "Characterization of delamination in fiber-reinforced epoxy-based PCB laminates, using an EBG-enhanced planar microwave sensor," in *IEEE Trans. Compon. Packag. Manuf. Technol.*, vol. 7, no. 10, pp. 1739-1746, Oct. 2017.

[2] S. Kharkovsky and R. Zoughi, "Microwave and millimeter wave nondestructive testing and evaluation - Overview and recent advances," in *IEEE Instrum. Meas. Mag.*, vol. 10, no. 2, pp. 26-38, April 2007.

[3] K. Zhang, R. K. Amineh, Z. Dong and D. Nadler, "Microwave sensing of water quality," in *IEEE Access*, vol. 7, pp. 69481-69493, 2019.

[4] H. Wu, M. Ravan, R. Sharma, J. Patel, and R. K. Amineh, "Microwave holographic imaging of nonmetallic concentric pipes," *IEEE Trans. Instrum. Meas.*, vol. 69, no. 10, pp. 7594–7605, Oct. 2020.